Validation and Development of an Atmospheric Electroaerodynamic Propulsion System

Gaige Sidaway[1], Britain Steele[2], Tyler Zeringue[3], and Conner Evans[4]
Mississippi State University, Mississippi State, MS 39762, United States

Electroaerodynamic (EAD) propulsion has been extensively used for satellite propulsion and microchip cooling; however, only limited research has been conducted for aeronautical use of electroaerodynamics for propulsion. This paper reports on research conducted to construct a proof-of-concept model of an electroaerodynamic propulsion system and to validate several factors that could impact the thrust of such a system. Results were experimentally gathered to determine the effects on thrust by voltage and collector and emitter gap spacing. A test stand was constructed with a design that included interchangeable electrodes and a slide for gap spacing. Data was gathered using an anemometer to establish a trend showing that higher voltages equate to a larger thrust output. The highest airspeed achieved during testing was 3.00 m/s. The proof of concept demonstrated that utilization of electroaerodynamics for propulsion, particularly for UAVs, is possible, but further research will need to be done to explore the feasibility of the system. The trends determined in this report can help direct these future research initiatives.

I. Nomenclature

A	=	cross-sectional area
d	=	distance between electrodes
DC	=	direct current
E	=	electric field
F	=	thrust
V	=	electric potential
v	=	velocity
μ	=	ion mobility of the fluid

II. Introduction

With recent trends towards advanced air mobility and sustainable aviation, demand for quieter and more environmentally friendly aircraft propulsion systems has risen. One potential solution explored is electroaerodynamic (EAD) thrust, which utilizes momentum transfer between charged particles and air molecules. EAD propulsion has the unique benefit of having no moving mechanical parts or combustion, allowing it to be significantly quieter and environmentally cleaner than traditional aircraft propulsion mechanisms.

Electroaerodynamic propulsion, a process utilizing similar concepts as ionic thrusters in spacecraft, involves positioning an anode and cathode under high voltage to create an electric field and corona discharge. Under high voltage, ions move from the positive end, colliding with air molecules. This collision imparts momentum onto the air molecules, creating an ionic wind that imparts thrust, as depicted in Fig. 1 [1].

[1] Aerospace Engineering Department, Student Member, Undergraduate, 1604884
[2] Aerospace Engineering Department, Student Member, Undergraduate, 1281766
[3] Aerospace Engineering Department, Student Member, Undergraduate, 1400907
[4] Aerospace Engineering Department, Student Member, Undergraduate, 1604890

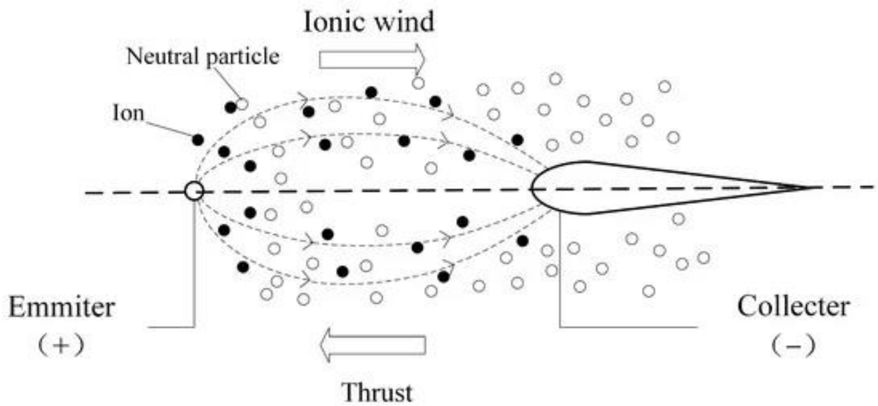

Fig. 1 Ionization of Ambient Air and momentum Exchange [1]

Ion propulsion technology has traditionally been employed in deep space exploration, due to its high specific impulse allowing for longer mission lifespans for a set propellant mass. However, ion propulsion or EAD principles see limited use in aeronautic applications due to its low overall thrust outputs. The current state of EAD design renders it impractical for sustained atmospheric flight, particularly for missions requiring high thrust or rapid acceleration. Nevertheless, researchers have been working on ways to optimize EAD systems and make the systems more practical for atmospheric flight. And while researchers have delved into exploring several optimization factors such as voltage or emitter and collector geometries, there is still significant research required to fill in the gaps in current industry knowledge.

Recent breakthroughs in EAD research, such as Steven Barrett of MIT and his team's achievement of creating a plane powered by ionic wind, have renewed interest in optimizing EAD systems for practical flight [2]. Challenges, however, persist, as evidenced by the MIT-developed plane's reliance on a slingshot for initial takeoff, revealing practical hurdles in implementing ion propulsion for atmospheric flight.

III. Literature Review

A. Electroaerodynamic Propulsion

Ion propulsion systems rely on electrons traveling across a distance, exchanging momentum between ions and the ambient atmospheric gases from the cathode to the anode. This process creates a corona discharge between an emitter (a sharp electrode) and a collector (a grounded or negatively charged, blunt electrode). The thrust generated by this system is governed by current (I), distance between electrodes (d), and the ion mobility of the air (μ) [3]. The relationship is shown in Eq. (1).

$$F = \frac{Id}{\mu} \tag{1}$$

The EAD glider developed by MIT [2] has recently implemented a new concept using wire emitters and airfoil collectors for a wire-to-airfoil setup. This setup enables the collector to generate lift by accelerating air using momentum exchange between ions and ambient atmospheric gases. As a result, the aircraft requires less thrust since the collectors provide the lift. Furthermore, EAD concepts have also been used in the electronics industry in the form of small-scale system cooling devices.

B. Expectations Derived from Academic Journals

Analyzing trends in electroaerodynamic thrust systems involves understanding previous literature and research to improve the performance of ionic engines. Researchers have identified a relationship between several variables, such as ion mobility, electrode configuration, voltage-current relationships, and electrode spacing, that affect the thrust production from EAD systems. By better understanding these variables, the ability to manipulate and improve EAD systems becomes more achievable.

Previous research has shown that increased electrode spacing generally leads to increased thrust readings. However, there is a critical distance where the system no longer produces thrust. For instance, in Ref. [3], an optimal spacing between 57 to 70 mm was projected for the pin emitter. Thus, it is crucial to calibrate each system to ensure electrode spacings are optimized for maximum thrust output.

Comparative analysis of varying geometries within EAD systems has been relatively rare. However, NASA research in Ref. [3] demonstrated a significant relationship between needles, the number of pins, the spacing between them, and the electric field within the system. The optimum spacing between points was 29 mm for a gap spacing of 50 mm. Adding more emitters at this spacing range improved the thrust produced, but the system required more power at a higher rate than the increase in thrust, showing diminishing returns.

Furthermore, different emitter geometries and configurations can impact the aerodynamic performance of EAD systems. Therefore, it is essential to explore ways to maximize the amount of ionized air and increase the amount of current flowing through the system while minimizing the drag placed on it. Various emitter geometries can help achieve these goals. While increasing the voltage in the system can benefit the amount of thrust produced to some extent, it is essential to note that as the voltage increases, the electric field surrounding the system also increases, which can eventually lead to arcing. Arcing can cause significant losses in the system due to energy losses from light, noise, and heat produced. Therefore, it is best to determine the ideal voltage for the system to ensure that arcing does not occur.

IV. Procedure/Methodology

The primary goal of the experimental phase for this project was to investigate the effect of several variables on an EAD thruster system's thrust output and to determine methods for optimization. A set of experiments was conducted to evaluate the impact of each variable. These experiments involved systematic alterations of each variable while maintaining a controlled testing environment to document thrust outputs accurately.

A. Design of Experiments/Variables

Three variables were examined to increase thrust: the shape of the emitter, the gap spacing between the emitter and the collector, and the voltage input to the emitter. Firstly, wire designs and sawtooth-tipped rings were considered the two main types of shapes for the emitter. Both designs have sharp edges that allow for better flow of electrons from the emitter. After much consideration, it was determined that the wire design provided a smaller flow area of air ionization within the testing bay. Looking at Eq. (2), the thrust produced by the system depends on the air's velocity and flow area [4].

$$F = \dot{m}_e V_e - \dot{m}_0 V_0 + (P_e - P_0) A_e \tag{2}$$

A horizontal wire setup gives the same airflow as a sawtooth setup with a smaller flow area, so the horizontal wires were not manufactured or tested within the timeframe of this report. For the sawtooth-edged ring, a serrated ring was used to optimize the amount of thrust produced by the system. A collector was created to correspond to the emitter's ring design by modifying the cross-section of a NACA-0012 air foil to fit copper tubing at its leading edge as seen in Fig. 2 below, ensuring that the air surrounding the circumference was ionized and the wind created experienced minimal turbulence over the collector.

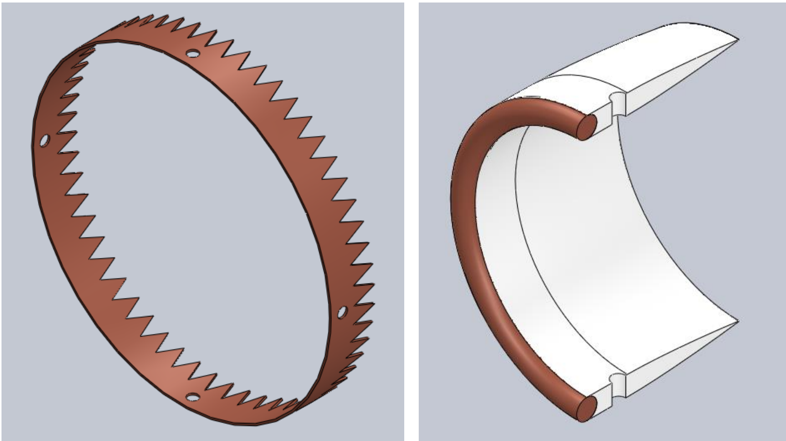

Fig. 2 Sawtooth Emitter Geometry (left) and the Section View of the Collector (right)

Spacing between the emitters and collectors was also examined. The spacing range tested from 5.283 mm to 34.59 mm between the emitter's back end and the collector's front end. The spacing was varied by turning a knob which increased or decreased the spacing by 1.041 mm intervals by moving the emitter along a slide while keeping the collector location constant. By gathering this data, two important data points were captured: the trend between spacing and thrust and the optimal gap spacing for maximum thrust.

The experiment's final independent variable was the emitter's voltage input. The voltage was varied by using a voltage amplifier. The input voltage was tested at 3, 4.5, and 6 volts since this was the range allowed by the voltage amplifier used, and the output voltage from the amplifier was measured throughout testing. The voltage was also tested at 6, 9, and 12 volts with a higher rated voltage amplifier. The varying input voltages were tested during each incremental change in gap spacing to determine which voltage and gap spacing combination was most effective at producing wind speed. Three tests were performed with finer incremental changes in gap spacing to more accurately determine the optimal distance.

B. Experimental Setup

To perform experimentation safely and consistently, a test stand was built to house the emitter and collector, as seen in Fig. 3. The test stand was constructed to have a wooden base topped by an acrylic tube housing for the corona area. The acrylic was manufactured to open on hinges to provide better access to the emitter and collector within. The emitter and collectors were detachable to allow for parts to be interchanged between tests if needed. The emitter was attached to a movable stand that was threaded to allow for movement of the stand with the twist of a knob. Each complete rotation of the knob would move the emitter 1.041 mm along the track. Wires were attached directly to the emitter and collector and run to a step-up power module which was attached to a variable voltage source. The electrical system supplied high voltage, low current DC power to the system.

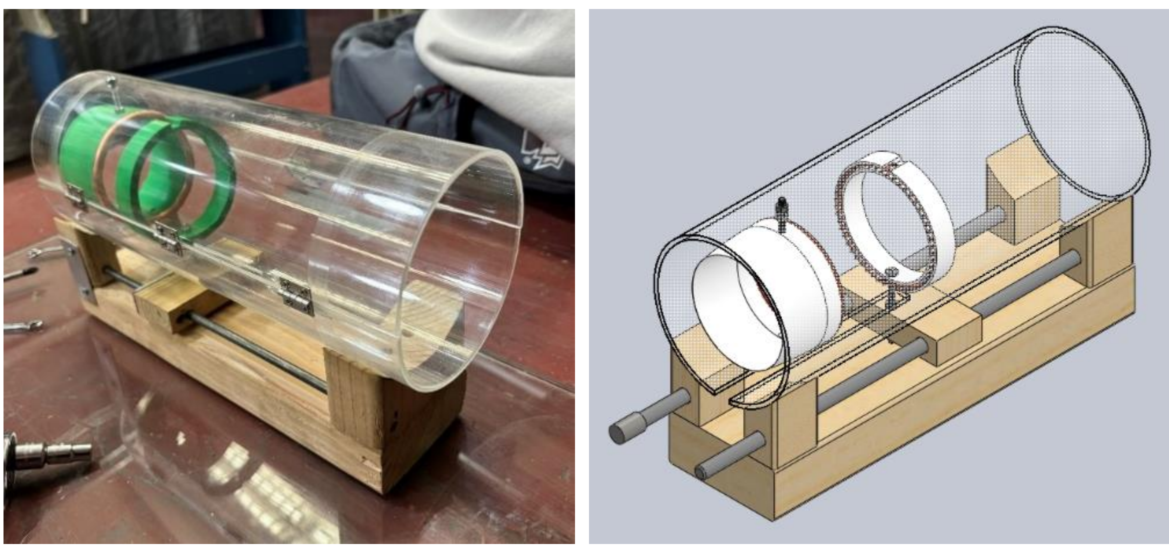

Fig. 3 Testing Stand (left) and SolidWorks Model (right)

To collect data during the experiment, several devices were also used in conjunction with the test stand. An anemometer was located to the exit of the acrylic tube to measure the wind speed at the exit. A high voltage meter comprised of a voltage divider and a kilovolt reader was attached to the electrical wiring inputting voltage to the emitter. The meter displayed the voltage in kilovolts during testing. To measure gap spacing, the number of rotations of the knob controlling the emitter track movement was recorded. Figure 4 shows an image of test day setup.

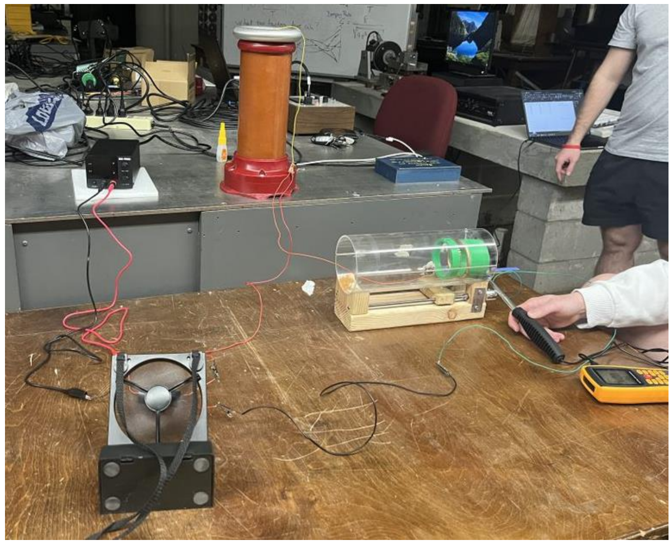

Fig. 4 Testing Setup

All testing conducted followed specific steps outlined in test procedure cards created for the experiment. To summarize the test procedure, data was recorded in sweeps. During each sweep, the emitter and collector types were kept constant. The first sweep for each combination of emitter and collector began with a gap spacing of 10 rotations (11.531 mm) between the emitter and collector. The system was turned on and data (voltage, spacing, and airflow speed) was collected for 3-, 4.5-, 6-, 9-, and 12-volt inputs at this gap spacing. Then gap spacing was increased by 5.283 mm and data collection was repeated. This process was repeated until the spacing became too large for electron flow between the emitter and collector. Subsequent sweeps were then repeated at smaller increments of gap spacing.

C. Data Collection

During the tests, measures were taken to prevent any disturbances in flow that could compromise the accurate calculation of system-produced thrust. An anemometer captured wind speed and a scale aided in approximating thrust output. The wind speed data gathered through the anemometer was utilized to compute thrust using Eq. (2). This equation relies on mass flow rate calculations derived from density and volume flow rate, which, as stated earlier, suggests that the higher the flow area, the higher the thrust produced.

The scale was utilized in testing by placing the system on the scale and comparing the difference in force displayed with the EAD system on and off. During the initial testing the weight scale used to measure thrust was not sensitive enough to read the forces applied to the scale. Testing proceeded by measuring air speed exclusively. After reattempting thrust measurements using the scale with the 9-volt testing, thrust values were collected successfully for three distances. These measurements were used in Eq. (2) to calculate the area of the airflow produced. With this calculated flow area, the thrust was able to be calculated for all airspeed measurements.

The anemometer was used to determine the wind speed at the exit of the testing stand by placing the fan of the anemometer at the highest wind speed location. The anemometer was set to display the max value it received, and the max value was recorded in Microsoft Excel as the highest velocity reading. The resulting values were used to plot distance vs velocity to produce the results below.

V. Results

The EAD thrust testing bay was subjected to 3 tests to investigate the maximum thrust the system can produce. It is important to note that thrust was calculated using Eq. (2), where velocity was measured using an anemometer, and flow area was calculated by placing the system vertically on a scale and seeing how much force it applies to the scale. Three test points were averaged to get the results. The average scale reading was 1.5667 g or 0.0154 N. Using this applied force and the averaged airspeed of 2.4413, flow area was calculated to be 0.0021 m^2. This value was used to calculate thrust for the testing shown below. The data collected is visualized below, showing the system's capabilities throughout each test.

A. Test 1: 3V, 4.5V, and 6V Input

For the initial test, input voltages of 3, 4.5, and 6 volts were tested every 5.283 mm until the system was no longer capable of producing thrust. Afterwards, the maximum thrust possible to achieve was calculated. Then airspeed, thrust, and output voltages were graphed to their corresponding voltages and compared in Fig. 5.

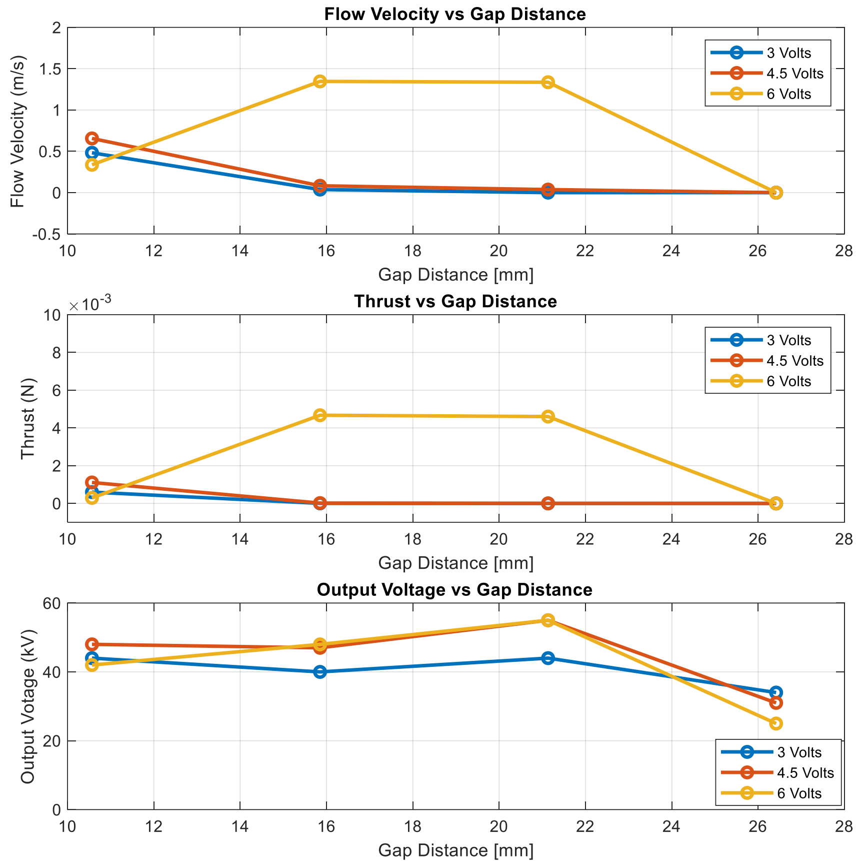

Fig. 5 Graph showing Flow Velocity, Maximum Thrust, and Voltage Output vs Gap Distance respectively during Test 1

The data above revealed a few important points. First, the data showed that ionization and, in turn, thrust was produced at much smaller distances than were anticipated. With a smaller distance capability, the 5.283 mm testing increments produced too small of a data set to determine a trend from Fig. 5. The maximum thrust produced by the system occurred between 16 and 22 mm, emphasizing that the changes in gap spacing needed to be smaller to provide more data points. While this first test did achieve the goal of constructing a functional proof-of-concept design, the increments for gap spacing measured were too large. For these reasons, another test was performed.

B. Test 2: 6V, 9V, and 12V Input

A second test was performed in the same manner as Test 1 with data being collected every 1.041 mm for voltages of 6-, 9-, and 12-volt inputs. This test resulted in output voltages closer to 100kV. The data is collected and visualized in Fig. 6 below.

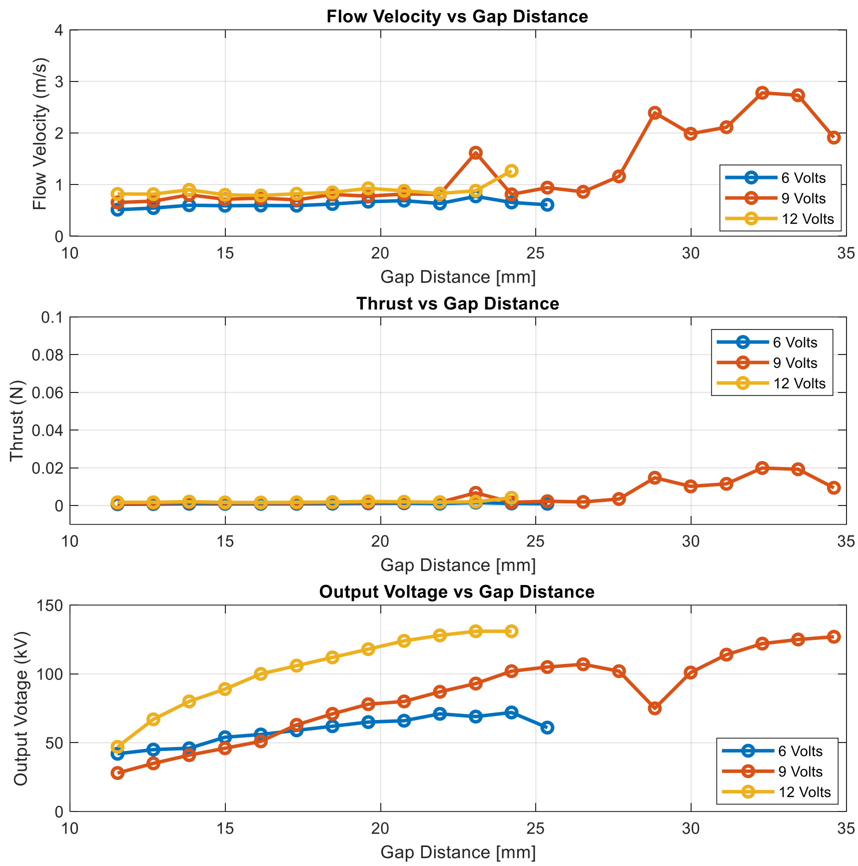

Fig. 6 Graph showing Flow Velocity, Maximum Thrust, and Voltage Output vs Gap Distance respectively during Test 2

After refining sweep increment to 1 rotation, the data shown in Fig. 6 gives an enhanced view of the data collected in Fig. 4 and reveals optimal spacing for maximum thrust production.

C. Test 3: 9V and 12V Input

The final test was performed in the same manner as Test 1 and 2 with data being collected every 1.041 mm. The 6-volt input was omitted since it has been established that maximum thrust occurs with a higher input voltage. Test 3 consisted of testing higher input voltages 9- and 12-volts and this test resulted in output voltages closer to 100kV. The data is collected and visualized in the figure below.

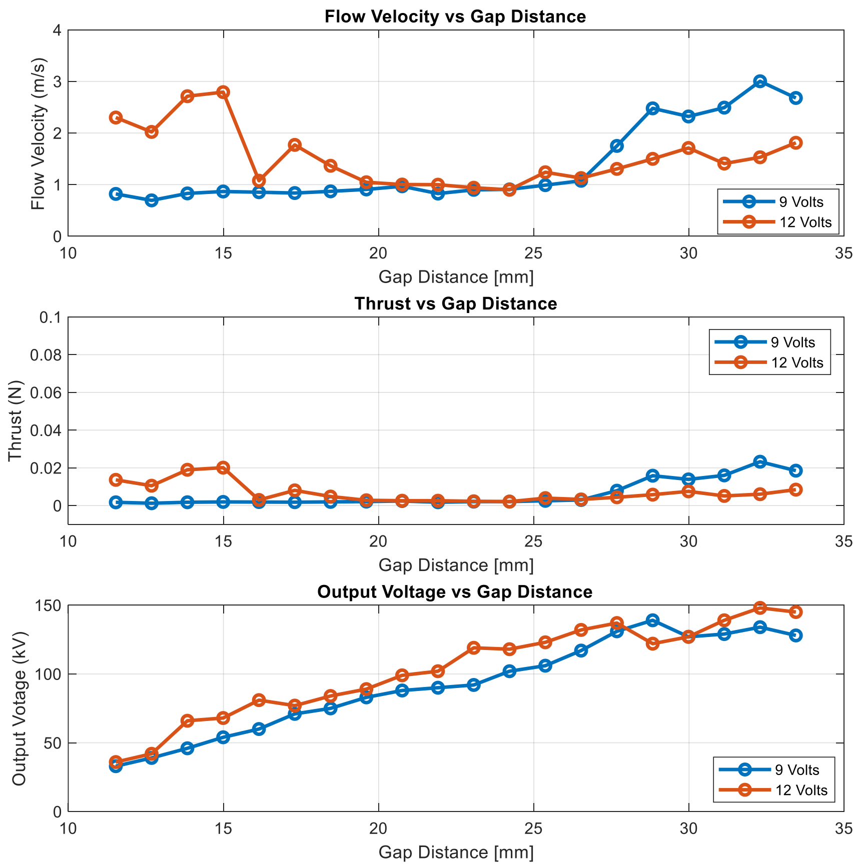

Fig. 7 Graph showing Flow Velocity, Maximum Thrust, and Voltage Output vs Gap Distance respectively during Test 3

The data shown in Fig. 7 for test 3 appears consistent with the data shown in Fig. 6 for test 2, reinforcing the claim that an optimal spacing between an emitter and collector exists.

VI. Discussion

Figure 5 shows the first test of the EAD thruster and its actual capabilities. More importantly, this test gives information on the range of ionization that the system can operate in and the difference that current has on the experiment's results. With this test, there was an expectation that the electrode spacing could reach as far as 150 mm (6 inches), causing the initial test to collect fewer data points than intended. Additionally, the input voltage was intentionally varied throughout the test. Still, it had virtually no effect on the output voltage of the step-up power module, concluding that raising the voltage decreased the current while maintaining power in the system. This lower current is directly proportional to a decrease in thrust as shown in Eq. (1), proving that higher voltage means a more powerful EAD thruster.

Figure 6 established optimal spacings exist for higher voltages and show relationships to gap spacing and the production of higher thrust from the system, and Figure 7 reinforced these findings with more data consistently showing an optimal exists.

The primary purpose of the testing stand that was manufactured and tested above was to determine the optimal spacing and voltage needed to maximize the thrust produced by an EAD thruster. Based on the information presented, the thrust of an EAD thruster can be optimized by maximizing flow area within the system, placing the electrodes 33-45 mm apart, and having at least a 9-volt input into a 40 kV step-up power module. However, more variables must be explored to ensure that the system produces maximum thrust, leaving room for further research.

Areas to explore in future optimization of EAD thrusters include varying output voltage and emitter point spacing. Output voltage could be explored to help maximize emitter spacing and current flow through the system since both are expected to proportionately increase thrust. By varying emitter spacing, there is a potential to maximize the ionized area in the system and help to increase thrust. Lastly, ways to increase the mass flow rate to the system through an increase in flow area will help to increase thrust. A potential way to do this would be to use the EAD thruster as a turboshaft to power a propeller. This could help to increase airflow in the system and significantly increase the mass flow rate for an EAD thruster.

VII. Conclusion

This research achieved its goals of manufacturing a proof-of-concept EAD system and validating computational trends for influencing thrust output. The research support trends that help to determine optimal electrode gap spacing and voltage in an EAD system. The research concluded that EAD propulsion has the potential to be used in the aviation industry; however, it was also observed that an EAD system has a low overall thrust output. The current limitations on thrust will likely influence EAD technology to be used more for small-scale aviation needs such as for UAVs.

Future research could be conducted using various emitter and collector geometries with the goal of reaffirming the trends presented in this paper as well as determining the optimal values for each unique system. Also, to make EAD systems more practically viable, extensive research into optimizing thrust output should be conducted. One potential topic for optimizing thrust could be to research methods for minimizing energy losses due to sound, light, and heat produced by the system during arcing and corona discharge.

Acknowledgments

The authors of this report would like to thank Rob Wolz and Carmen Sescu for their advice throughout the project, Mike Newman and the Center for Advanced Vehicular Systems for allowing for the use of equipment and for assistance with waterjet cutting of metallic parts, David Wallace for advice and the use of high voltage meter equipment, Brandon Warner for assistance with test stand manufacturing and using equipment, and the National Space Grant Foundation for grant funding.

References

[1] Lin, T., Huo, M., Qi, N., Wang, J., Wang, T., Gu, H., Zhang, Y., "Coupling Dynamics and Three-Dimensional Trajectory Optimization of an Unmanned Aerial Vehicle Propelled by Electroaerodynamic Thrusters," *Aerospace* [online journal], Vol. 10, Paper 950, 2023, URL: https://doi.org/10.3390/aerospace10110950.

[2] Xu, H., He, Y., Strobel, K. L., Gilmore, C. K., Kelley, S. P., Hennick, C. C., Sebastian, T., Woolston, M. R., Perreault, D. J., Barrett, S. R. H., "Flight of an aeroplane with solid-state propulsion," *Nature* [online journal], Vol. 563, 2018, pp. 532–535, URL: https://doi.org/10.1038/s41586-018-0707-9.

[3] Wilson, J., Perkins, H. D., and Thompson, W. K., "An Investigation of Ionic Wind Propulsion," 2009, pp. 5, 9. URL: https://ntrs.nasa.gov/api/citations/20100000021/downloads/20100000021.pdf.

[4] Benson, T., "General Thrust Equation," 2021. URL: https://www1.grc.nasa.gov/beginners-guide-to-aeronautics/rocket-thrust-equation/